

# Electrical Study of Changes in Impedance and Internal Parameters of Nano Structures of Molybdenum Disulfide Semiconductor Type (MoS<sub>2</sub>-2H/3R) with Changes in Temperature

Hussein AlHussein<sup>a,\*</sup> , Jamal AlSharr<sup>a</sup>, Hasan AlKhamisy<sup>b</sup> 

<sup>a</sup>Department of Physics, faculty of Science, University of Aleppo, Syria,

<sup>b</sup>Institute of Health Technology, University of Aleppo, Syria.

## Keywords:

MoS<sub>2</sub>  
Zeta sizer nano series  
Impedance  
Electronic traps  
Electric charge carriers  
Activation energy  
Atomic force microscopy (AFM)

## ABSTRACT

MoS<sub>2</sub> nanostructures were prepared using the hydrothermal method by reacting ammonium heptamolybdate tetrahydrate ((NH<sub>4</sub>)<sub>6</sub>Mo<sub>7</sub>O<sub>24</sub>·4H<sub>2</sub>O) with citric acid monohydrate (C<sub>6</sub>H<sub>8</sub>O<sub>7</sub>·H<sub>2</sub>O) in distilled water with the presence of sodium sulfide (Na<sub>2</sub>S), we have found from the Arenos diagram that the value of the activation energy of (MoS<sub>2</sub>-2H/3R) is low and equal to  $E_a = 0.0505$  (e.V). From the atomic force microscope (AFM) images, we found that the size of the surface aggregates of the sample (table - MoS<sub>2</sub>-2H/3R) ranges between (100-150) nm. From studying the changes in the impedance with different temperatures ( $T = 15, 30, \text{ and } 60$ ), we found that impedance is inversely proportional to both the applied frequency and the temperature, and at the frequencies the response corresponding to the temperature reaches a value of ( $Z = 20 \text{ K.}\Omega, T = 15^\circ\text{C}$ ). ) and at temperature ( $Z = 8.02 \text{ K.}\Omega, T = 30^\circ\text{C}$ ), and at ( $Z = 17.1 \text{ K.}\Omega, T = 60^\circ\text{C}$ ). It has been shown that the number of electric charge carriers ( $N_d$ ) increases with increasing temperature. On the contrary, we found a decrease in the number of electronic traps ( $N_s$ ) and a decrease in the relaxation time  $\tau_P$  with increasing temperature.

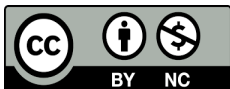
## Corresponding author:

Hussein AlHussein  
E-mail: [husionphy990@gmail.com](mailto:husionphy990@gmail.com)

Received: 10 March 2024

Revised: 16 April 2024

Accepted: 5 June 2024



© 2024 Published by Faculty of Engineering

## 1. INTRODUCTION

Molybdenum disulfide exists in layers stacked on top of each other, bound together by van der Waals forces. Whereas, in each layer of molybdenum disulfide, the molybdenum layer

is sandwiched between two layers of sulfur, Molybdenum disulfide (MoS<sub>2</sub>) is considered an effective semiconductor nanomaterial, but it is a very sensitive semiconductor material. There are many factors that affect its electronic structure and structural composition, including

the local coordination mechanism of molybdenum, sulfur vacancies, surface defects, and the crystal phase (1T 3R, 2H,), as well as the temperature of exfoliation, size and shape of the nanosheets, as this wide range of factors affecting the molecular and electronic structure and active surface area has led to many contradictory reports about the electrical.

Catalytic and optical properties of the material and thus its properties are completely different according to these three main phases [1]. The structure of molybdenum disulfide of crystal type (2H, 3R) is a trigonal prismatic arrangement, where the molybdenum disulfide crystal of type (3R) is characterized by the presence of a central molybdenum atom in the prismatic arrangement and is bonded with three sulfur atoms from the top and three atoms from the bottom [2], molybdenum disulfide (MoS<sub>2</sub>-2H/3R) is characterized by the possibility of the absence of reversible symmetry in its crystalline structure, as the absence of this factor generates a new set of nonlinear physical properties, including high light absorption[3, 4], which increases with increasing the number of individual layers in (MoS<sub>2</sub>-2H/3R) also causes Changes in the structure of the electronic levels, and thus this affects the distribution of electrons on both sides of the Fermi level, and thus the electronic levels and electrical properties, where as a result of the crystal stacking, the prismatic structures meet in a hexagonal shape, forming a honeycomb structure is stackable and is of the (hcp) type, This feature contributes to the important electrical and electronic properties of (MoS<sub>2</sub>-2H/3R)[5].

## 2. THE IMPORTANCE OF RESEARCH

The importance of the research is evident in studying the effect of temperature changes on the electrical properties and electrical and electronic behavior of nanostructures with crystalline patterns (MoS<sub>2</sub>- 2H/3R) in order to complete the electrical characterization of the three patterns (3R, 2H, 1T), where atomic layers and thin films with the pattern are distinguished (1T) with superconductivity, which is the focus of research in the next stages.

## 3. MATERIALS USED, METHOD AND STAGES OF PREPARATION AND EXPERIMENTAL RESULTS

### 3.1 Materials used

Ammonium Heptamolybdate Tetrahydrate ((NH<sub>4</sub>)<sub>6</sub>Mo<sub>7</sub>O<sub>24</sub> · 4H<sub>2</sub>O), Tetrathiomolybdate Ammonium, Distilled water, citric acid monohydrate (C<sub>6</sub>H<sub>8</sub>O<sub>7</sub> · H<sub>2</sub>O), Na<sub>2</sub>S.

### 3.2 Method of preparation

To prepare nanostructures from (MoS<sub>2</sub>-2H/3R), the preparation process was carried out using the hydrothermal method [6,7], where in the manufacturing process sodium sulfide was used as a source of sulfur in order to obtain molybdenum sulfide, With the only difference being the processing time in the autoclave to prepare MoS<sub>2</sub>, for prepare the pattern (MoS<sub>2</sub>-3R) the reaction time was 4 hours at 200°C with the presence of sufficient (excess) amounts of sulfur. As for preparing the pattern (MoS<sub>2</sub>-3R/2H) we doubled the reaction time. Up to 12 hours at a temperature of 200°C and thus we have obtained a pure powder of Molybdenum sulfide as shown in Figure (1). Where we pressed an amount of this powder amounting to (M = 1gr), we obtained a (MoS<sub>2</sub>-2H/3R -Tablet) with a diameter of (15 mm) and a thickness of (2mm) for the electrical characterization, using a hydraulic compressor with a capacity of (5 ton/cm<sup>2</sup>), and without heat treatment (the tablets have not been heat treated).

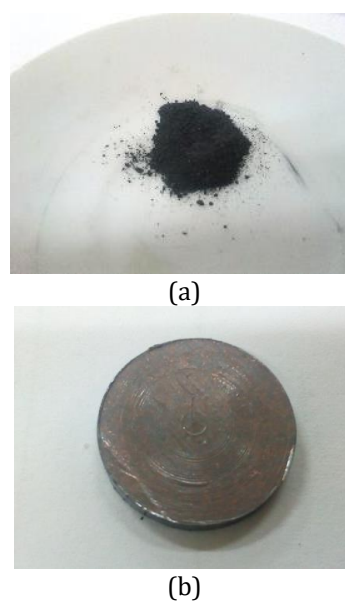


**Fig. 1.** (a) Pure powder prepared from (MoS<sub>2</sub> - 2H/3R), (b) (MoS<sub>2</sub> - 2H/3R) tablets.

### 3.3 X-ray diffraction spectrum

In order to verify the structure of the prepared molybdenum disulfide, the crystallization of the prepared samples was studied by using an X-ray device produced by Phywe company and applying a current which intensity is (0.1 mA and an angle hop of (0.1 degrees every 10 sec)) measurements between angles (80°-10°) were taken and a copper anode which wavelength is of was used (1.541 Å).

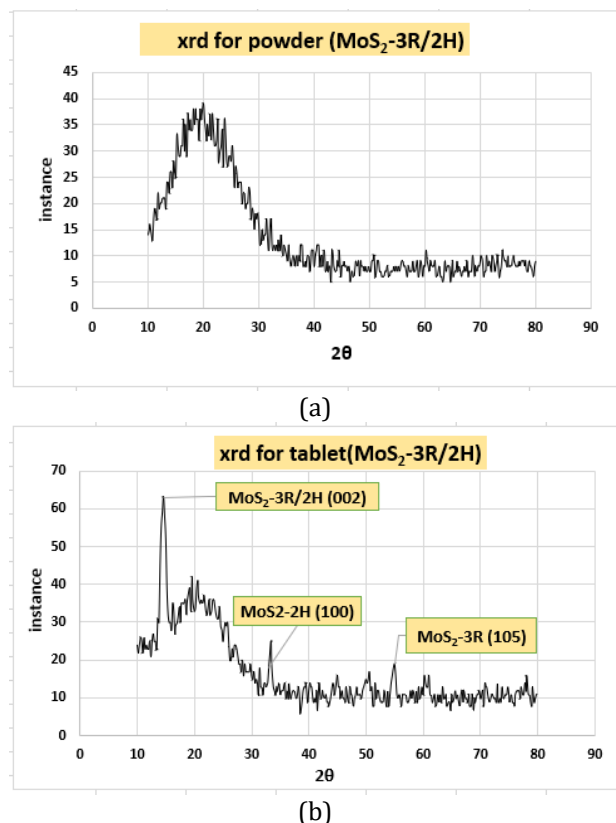


**Fig. 2.** (a) XRD of nano powder prepared from (MoS<sub>2</sub> - 2H/3R), (b) XRD of tablet (MoS<sub>2</sub> -2H/3R).

X-ray spectra (XRD) of the nano powder prepared from MoS<sub>2</sub> showed that there are no clear peaks, and this indicates and confirms the nanostructure of MoS<sub>2</sub> is amorphous, and this is consistent with the data of the card (JCPDS No.06-0097) [8], as in Figure (2-a). Since the crystallization process in the patterns (3R, 2H) is related to pressure and the degree of oxidation, we prepared tablets with diameters of (1.5 cm and thickness of (3 mm from (powder-MoS<sub>2</sub>.2H/3R) using a hydraulic compressor by subjecting (powder-MoS<sub>2</sub>) to a pressure of (5 ton), The X-ray diffraction measurements of these discs showed the presence of a very clear and intense peak corresponding to the

crystalline plane (002) corresponding to the degree (2θ = 14.6°). This is consistent with the values of the aforementioned molybdenum disulfide reference cards. Figure (2-b) shows the presence of several diffraction peaks, which means that there are several phases within the structure of (MoS<sub>2</sub>-2H/3R).

**Table 1.** shows the diffraction angles and corresponding crystal planes.

2θ	14.6	32.5	50
(Hkl)	(002)	(100)	(105)
Pattern	2H/3R/1T	2H	3R

The (002) crystal plane, which is the preferred crystal plane for MoS<sub>2</sub> crystals, is as shown in Figure (3-b). Depending on Bragg's law of the diffraction of X-rays as in relation (1), the distance between the crystal planes defined by Miller's indices (hkl) can be set:

$$2d_{hkl} \sin(\theta_{hkl}) = n\lambda \quad (1)$$

Where:  $d_{hkl}$  represents the distance between the parallel crystal planes according to the hkl direction, and the angle ( $\theta_{hkl}$ ): is the diffraction angle, and  $n$ : is the diffraction rank,  $\lambda$ : represents the wavelength of the X-rays ( $\lambda = 1.541 \text{ \AA}$ ) By calculation, it turns out that the value of the lattice constant is ( $d_{hkl} = 5.906 \text{ \AA}$ ), And the value of lattice constants ( $a$ ) is calculated from relation (2):

$$d_{hkl} = \frac{a}{\sqrt{h^2+k^2+l^2}} \quad (2)$$

### 3.4 Studying the surface structure of molybdenum disulfide ((MoS<sub>2</sub> -2H/3R) - Tablet) using AFM atomic force microscopy

Using atomic force microscopy AFM, a microscopic picture of the surface of the tablets prepared from molybdenum sulfide powder (MoS<sub>2</sub>-Tablet) was taken, where we used different sizes and the same area and of the sample surface, (1.01µm × 1.01µm).

These images showed the shape of the surface atomic clusters on the surface, where the average size of the atomic clusters formed in the structure of the surface of the (MoS<sub>2</sub>-2H/3R -Tablet) was determined, as the formed sizes ranged between (100-150) nm as shown in Figure (3), where the crystalline phases of MoS<sub>2</sub> are formed under the process of hydraulic pressure.

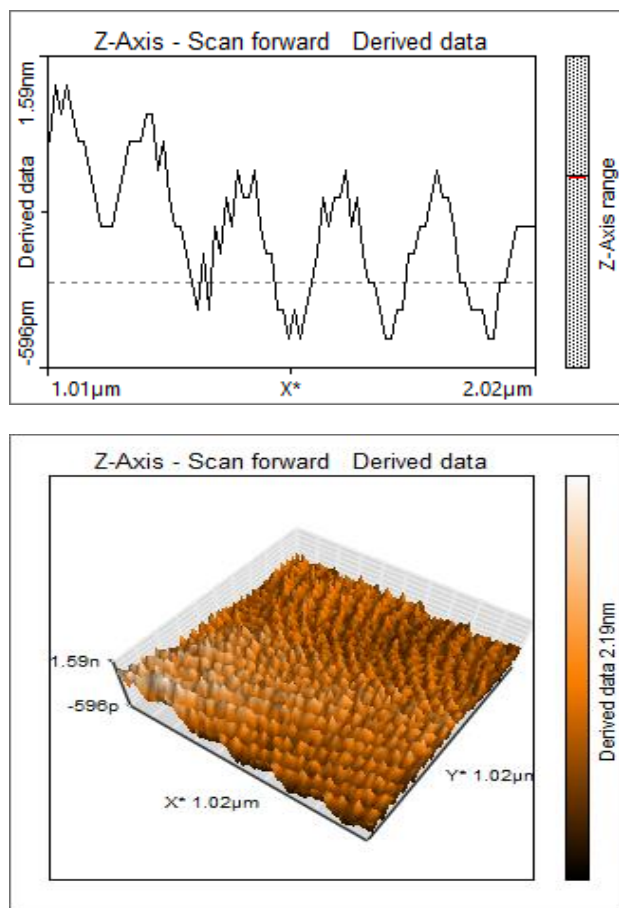


**Fig. 3.** AFM images of tablet molybdenum disulfide at two scales (1.02μm×1.02μm).

### 3.5 Measurements (Zetasizer Nano Series) of formed nanoparticles (MoS<sub>2</sub>-2H/3R)

To find out the size of the formed nanoparticles, we measured the size of these granules using the Zetasizer Nano device, model ZS-Nano, produced by Malvern Company, using a red laser source, with a wavelength of (632.8 nm), we placed a suspension of molybdenum sulfide (MoS<sub>2</sub> -2H/3R) in quartz cells designated for the device, the device is calibrated at a constant temperature of (25 °C), and the dimensions of the scanned cell are (5.5) m.m, and a count rate of (141.8=count rate (kcps)), so we found that the particle sizes ranged from (150-350) nm as shown in the following figure (4).

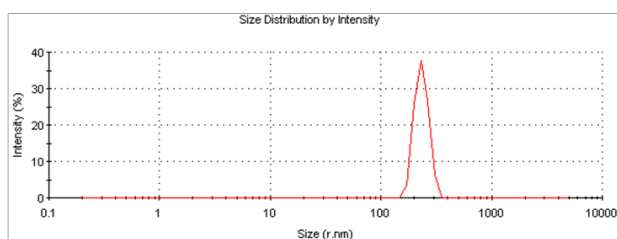


**Fig. 4.** Zetasizer Nano Series measurements of the size of the prepared MoS<sub>2</sub> granules.

### 3.6 Measuring the impedance spectrum of Molybdenum disulfide (MoS<sub>2</sub> -2H/3R) - Tablet)

This spectrum helps us in characterizing the material in the (dynamic) state, from which we extract the response time of the material. In the end, we will deduce the (parameters) affecting the electrical behavior of the material. Alternating current is applied to both ends of the sample and the studied sample is connected to the GAIN PHASE ANALYZER (SI1253), with the detection resistance Rd as in Figure (5):

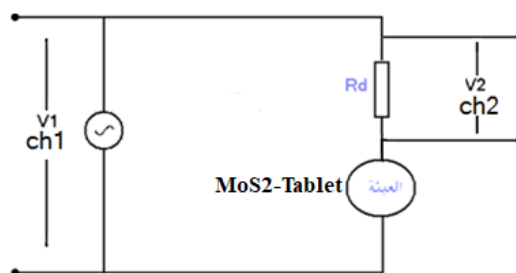


**Fig. 5.** A planning drawing shows the (MoS<sub>2</sub>-Tablet) method to measure its impedance.

Where a variable frequency alternating signal [100 Hz-20 kHz] is applied, with a fixed input potential (V1=5v) and the device measures the output potential V2 in its form, the transition function of the tested system System Under is measured. Therefore impedance is measured from the potential divider law, where this impedance is written by the relation (3):

$$Z(\omega) = R(\omega) + jX(\omega) \quad (3)$$

Which allows us to draw spectrum with the relationship (4):

$$X(\omega) = f(R(\omega)) \quad (4)$$

We plotted impedance spectrum (frequency response) of the sample ((MoS<sub>2</sub> -2H/3R) -Tablet) deduced by using a Solartron 125 phase gain analyzer, and obtained an arc of a circle. We studied the impedance spectrum of molybdenum disulfide (MoS<sub>2</sub>-2H/3R) Tablet by applying an alternating potential to the sample of (5 volts) and at different temperatures of (288, 303, 333) °K, where the curves appear in the form of arcs and parts of circle arcs, and this indicates that The equivalent circuit connected between each two grains consists of a variable resistance and a capacitor in parallel connected in series with a variable capacitor and another resistance. The impedance spectrum has been studied in three cases.

### 3.6.1 Spectrum of impedance of the Molybdenum disulfide (MoS<sub>2</sub>-2H/3R - Tablet) at a temperature: T = 15 °C

We have found the impedance spectrum of the Molybdenum disulfide changes  $X(\omega) = f(R(\omega))$ , and by applying frequencies ranging between (100hz-20KHz) and at the temperature  $t = 15^\circ\text{C}$ , it is part of the circle arch and taking the view of the circular part Regular, the value of the electrical resistance  $R(\omega) = R1 - R2$ , has been found, where: (R1; is the value of the primitive resistance, R2: the final resistance value),  $R(\omega) = 110 - 6.92 = 103 (K.\Omega)$ , as shown in Figure (6).

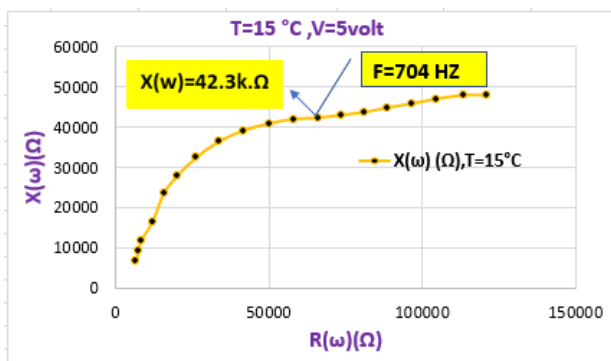


Fig. 6. Spectrum of impedance at the temperature T= 15 °C.

### 3.6.2 Study the frequency response of the real and imaginary part of the spectrum of impedance R(ω) at a temperature T = 15 °C

The changes of both  $R(\omega)$ ,  $X(\omega)$  are studied with applied frequencies (100Hz-20KHz) as shown in Figure (7).

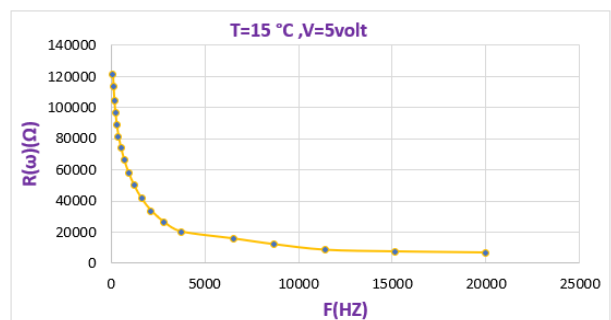


Fig. 7. Changes of the real part of impedance R (ω) with frequency F (HZ).

Where it becomes clear to us that the real part of the resistance decreases sharply from the value  $R = (120 - 20) K.\Omega$  to the value by means of increasing the frequency applied from low frequencies to (100 Hz – 400 KHz), and its changes are slight in the higher frequencies as the

value becomes  $R = 7 (K.\Omega)$  at high frequency  $F = (20) khz$ . As for the changes in the imaginative part  $X(\omega)$  of the impedance resistance, it indicates a gradual decrease of the value  $X(\omega)$  with the increase of the applied frequency as shown in Figure (8), where the value of the imaginary part decreases from the resistance to become  $x(\omega) = (50 - 9)K.\Omega$ .

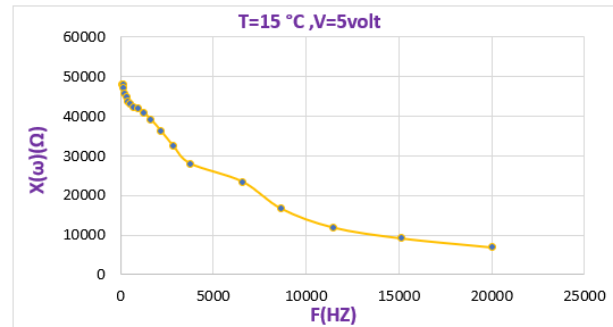


Fig. 8. Changes of imaginary part of impedance  $x(\omega)$  with frequency F (HZ).

### 3.6.3 Study of the impedance reluctance changes Z(Ω) with frequency F(HZ) at a temperature: T = 15 °C

Where impedance changes were studied at the same frequencies (100 HZ – 20KHz), where the changes of impedance that are severely decreasing ( $Z = 135 - 25 K.\Omega$ ) with an increase in the frequency until we have a frequency of ( $F = 100Hz - 400 HZ$ ) and then impedance changes become slight, as shown in Figure (9).

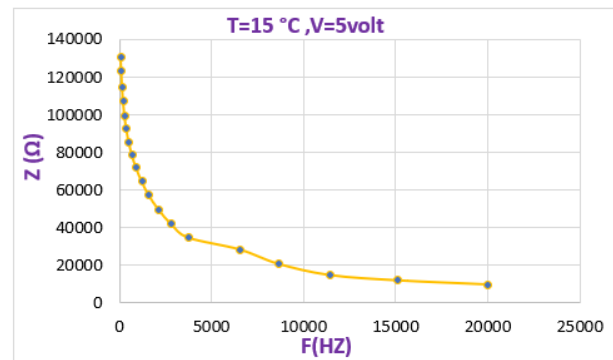
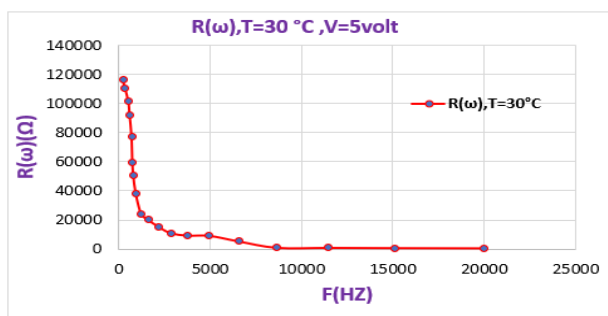


Fig. 9. Impedance reluctance changes Z (ω) with frequency F (HZ).

### 3.7. Studying the frequency response of the real and imaginary part of the impedance spectrum R(ω) at a temperature: T=30°C:

The changes of  $R(\omega)$  and  $x(\omega)$  were studied with the applied frequencies (100Hz-20KHz) as shown in Figure (10).



**Fig. 10.** Variations of the real part of the impedance  $R(\omega)$  with frequency  $F(\text{HZ})$ .

Where it turns out that the real part of the impedance resistance  $R(\omega)$  decreases sharply from the value  $R = (116) \text{ K}.\Omega$  to the value  $R(\omega) = (11.03) \text{ K}.\Omega$  with an increase in the applied frequency from low frequencies up to 100 Hz – 2840 Hz and the value of the real part  $R(\omega)$  continues to decrease to the value  $R(\omega) = (5.335) \text{ K}.\Omega$  and the resistance  $R(\omega)$  decreases to the value  $R(\omega) = (903) \Omega$  at frequency  $F = (8.664) \text{ kHz}$  and its changes become slight at higher frequencies, where the value of the real part of the impedance becomes  $R(\omega) = 720.4 \Omega$ . at frequency  $F = (15.133) \text{ kHz}$ , and the value of the real part of the impedance becomes  $R = (589.58) \Omega$  at the high frequency  $F = (20) \text{ kHz}$ , which is a very small resistance, and this means that the crystallized molybdenum disulfide can behave as a good and different conductor in the case of  $(\text{MoS}_2\text{-2H/3R})$  when subjected to high frequencies. As for the changes of the imaginary part  $x(\omega)$  of the resistance when applying an electrical potential of (5 volt) at a temperature  $(T=30^\circ\text{C})$ , it shows a gradual decrease in the value of  $x(\omega)$  with the increase in the applied frequency as shown in the figure, where the value of the imaginary part of impedance decreases from gradually to become  $x(\omega) = (41.170 - 11.47) \text{ K}.\Omega$  when the applied frequency increases from  $(F = 100\text{Hz} - 6.55\text{kHz})$  as shown in Figure (11).

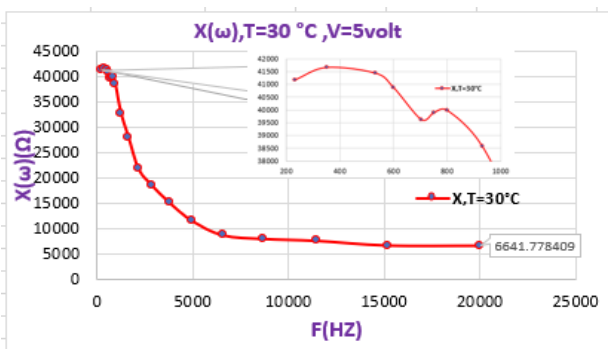


**Fig. 11.** Variations of the imaginary part of impedance  $X(\omega)$  with frequency  $F(\text{HZ})$ .

As for the frequencies  $F = 100\text{Hz} - 3.753\text{kHz}$ , we notice that the changes of the imaginary part of impedance become slight and range  $Z = (180 - 20) \text{ K}.\Omega$ , as shown in Figure (12).

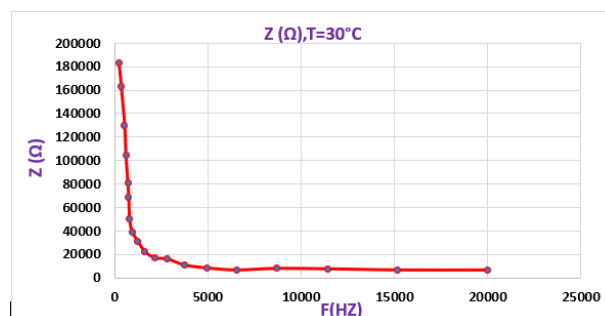


**Fig. 12.** Impedance  $Z(\Omega)$  changes with frequency  $F(\text{HZ})$ .

The impedance decreases gradually and slightly in the frequencies range of  $F = (3.75 - 6.55) \text{ kHz}$ , The specific impedance decreases to the value  $Z = (6.66) \text{ K}.\Omega$  at high frequencies  $(F = 20) \text{ kHz}$ .

### 3.8 Impedance Spectrum of Molybdenum Disulfide $(\text{MoS}_2\text{-2H/3R})$ at $T=60^\circ\text{C}$

The sample was placed in an oven of a type and the temperature was set at  $(T = 60^\circ\text{C})$  and by using the gain and phase analyzer device and applying a potential of  $(V = 5 \text{ volt})$ , the impedance spectrum was taken as in Figure (13), where the imaginary impedance part changes were studied. The with the real part of impedance according to the relation  $X(\omega) = f(R(\omega))$ , as shown in the figure (13).

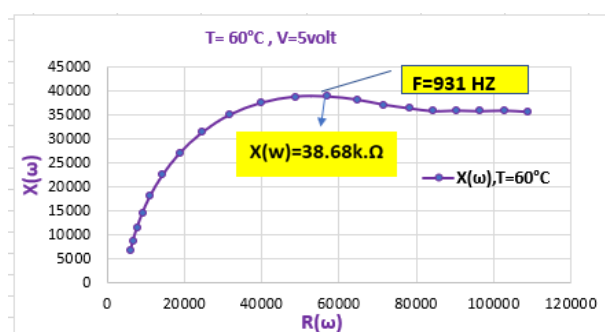


**Fig. 13.** The imaginary impedance part changes with the real part of impedance changes.

Where we found that the changes of the imaginary part with the real part are arcs of a circle and that the relation  $(\omega \times \tau_p = 1)$  is achieved at frequency  $F=931 \text{ HZ}$ . it is show that the changes in impedance spectrum of molybdenum disulfide  $X(\omega) = f(R(\omega))$  When applying frequencies ranging from  $(100\text{Hz} - 20\text{kHz})$  and at a temperature  $T = 60^\circ\text{C}$

it is part of a circle arc and by taking the part corresponding to the regular circular part, the electrical resistance  $R(\omega) = R2 - R1$ ,  $R(\omega) = 90 - 6.159 = 83.8 (K. \Omega)$  where: R1 is the value of the initial resistance, R2 is the value of the final resistance.

### 3.9 Studying the frequency response of the real and imaginary part of the impedance spectrum $R(\omega)$ at $T=60^\circ C$

The changes of  $R(\omega)$  and  $x(\omega)$  were studied with the applied frequencies (100Hz-20KHz) as shown in Figure (14).

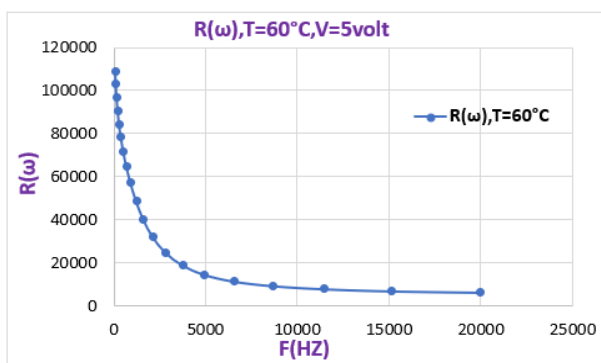


Fig. 14. Variations of the real part of the impedance  $R(\omega)$  with frequency  $F(HZ)$ .

It turns out that the values of the real part of impedance decrease sharply in the range of applied frequencies (100Hz – 4.96 KHz) to the value (108.9 – 14.41)  $K. \Omega$ , while at high frequencies (11.45 -20) KHz we notice that the values of the real part of the impedance becomes constant and ranges between (7.7 – 6.15)  $K. \Omega$ , As for the changes of the imaginary part  $X(\omega)$  of the resistance, it shows a gradual decrease in the value of  $X(\omega)$  with the increase in the applied frequency as shown in Figure (15), where the value of the imaginary part of the impedance decreases to become  $X(\omega) = (50 - 9) K. \Omega$ .

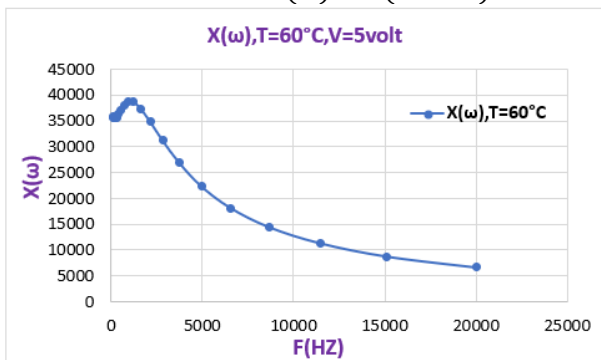


Fig. 15. Changes of the imaginary part of impedance  $x(\omega)$  with frequency  $F(HZ)$ .

It can be seen from the figure that the values of the imaginary part of the impedance increase in the range of low frequencies applied within the range (100Hz – 1.23 KHz), where the value of  $X(\omega)$  increases to the value 35.48 – 38.64 ( $K. \Omega$ ), and at higher frequencies applied within the range (20 – 2.14KHz), and we notice that the values of the impedance part are gradually decreasing according to the values (37.37 – 6.63)  $K. \Omega$ .

### 3.9.1 Studying the changes of impedance $Z (\Omega)$ with frequency $F (HZ)$ at $(T=60^\circ C)$

The impedance changes were studied at the same frequencies (100 Hz – 20KHz). we can see that the impedance changes are sharply decreasing  $Z = (114.6 - 26.57) K. \Omega$  with an increase in frequency to the frequency  $f = (100Hz - 4.96) KHz$ , as It is shown in Figure (16).

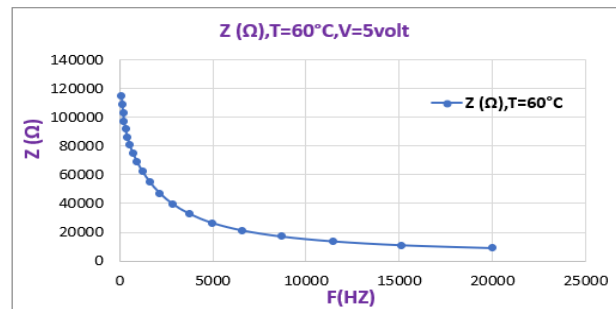


Fig. 16. impedance  $Z(\Omega)$  changes with frequency  $F(HZ)$

As for the higher frequencies within the range (6.55 – 20 KHz), impedance changes become slight and its value ranges from  $Z = (21.3 - 9.05) K. \Omega$ .

### 3.10 Comparing the changes of the impedance spectrum with temperatures of $(MoS_2-2H/3R)$

It can be seen from Figure (17) that the constant part of the changes of the imaginary part of the impedance becomes less valuable with increasing temperature in the order  $T = (15, 30, 60) ^\circ C$ ,  $X(\omega) = (48, 41.66, 35.6) K. \Omega$

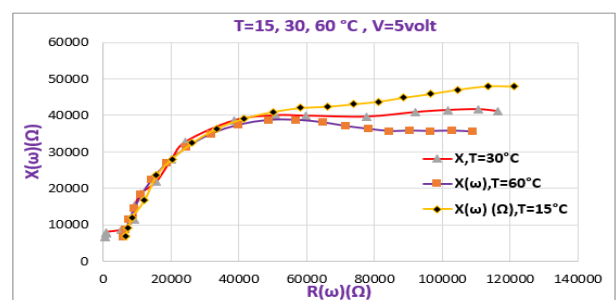


Fig. 17. Variation of impedance spectrum  $X(\omega)=f(R(\omega))$  with increasing temperature

When the temperature increases, we notice a shift of the frequency response peaks towards higher frequencies that verifies the relation  $\omega \times \tau_p = 1$ , which means a decrease in the life time of the charge carriers. The equivalent circuit with a parallel connection and the equivalent Randels circuit is given in the Figure (18).

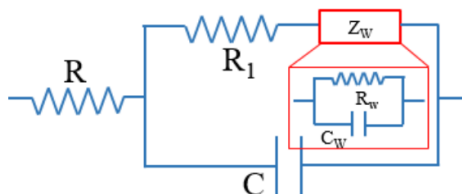


Fig. 18. Randels equivalent circuit.

### 3.11 Comparison of changes in the frequency response of the real part of the impedance spectrum, $R(\omega)$ , with increasing temperature

From Figure (19), we can see that the changes of the real part of the impedance become slight at high frequencies, which are higher than the frequency ( $F = 8664 \text{ Hz}$ ;  $8.66 \text{ KHz}$ ), as at this frequency and at a temperature ( $T = 15^\circ\text{C}$ ), the value of the real part of The impedance becomes equal to  $R(\omega) = 12127 \text{ }(\Omega) = 12.12(k.\Omega)$ .

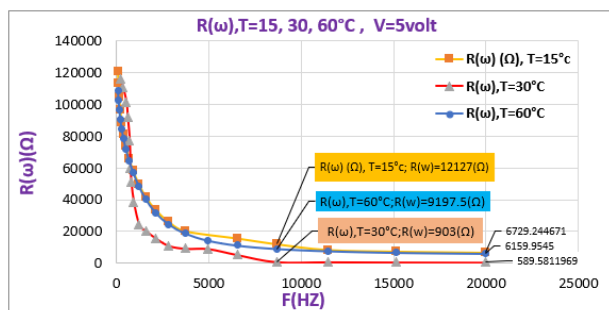


Fig. 19. Variations of the real part of impedance,  $R(\omega)$ , with changes in frequency ( $F$ ) and temperature ( $T$ ).

As for the temperature ( $T = 30^\circ\text{C}$ ), we note that the value of the real part of impedance corresponding to the frequency  $F = (8664 \text{ Hz}$ ;  $8.66 \text{ KHz}$ ) is equal to  $R(\omega) = 903 \text{ }(\Omega) = 0.930 \text{ (k.\Omega)}$ , while For the temperature ( $T=60^\circ\text{C}$ ), the value of the real part of impedance corresponding to the frequency  $F = (8664 \text{ Hz}$ ;  $8.66 \text{ KHz}$ ) is equal to  $R(\omega) = (9197.5) \text{ }(\Omega) = (9.1975) \text{ k.\Omega}$ . We can see from Figure (19) that molybdenum disulfide is suitable for electronic applications that require a temperature close to  $T = 30^\circ\text{C}$ , as it shows low resistance when subjected to high frequencies of the order of (10 KHz).

### 3.12 Comparison of the frequency response changes of the imaginary part of impedance spectrum $X(\omega)$ with increasing temperature

We notice from Figure (20) that the changes of the real part of impedance gradually decrease in low frequencies At The temperature is ( $T = 15^\circ\text{C}$ ), but at temperatures ( $T = 30, 60^\circ\text{C}$ ), we notice an increase in the value of the real part of the impedance at very low frequencies, and then it decreases with an increase in the applied frequency as shown in Figure (20). As for the high frequencies (20 KHz), we notice a decrease in the real part of the impedance at temperatures ( $15, 30, 60^\circ\text{C}$ ) to the same value  $R(\omega) = (6.6) \text{ K.\Omega}$ .

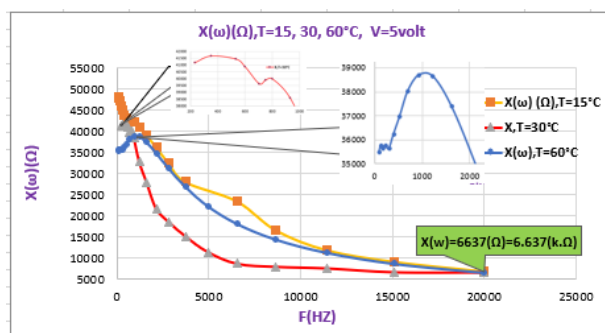


Fig. 20. Variations of the imaginary part of impedance  $X(\omega)$  with changes in frequency ( $F$ ) and temperature ( $T$ ).

### 3.13 Comparison the changes in the impedance $Z(\omega)$ with frequency change and with increased temperature

We note from Figure (21) that the changes of impedance with frequency are inverse changes as the impedance decreases with the increasing frequency applied as shown.

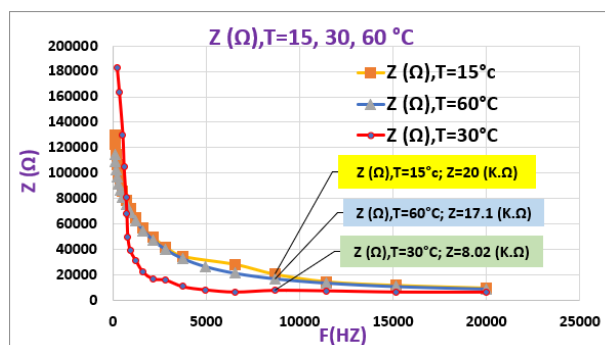


Fig. 21. impedance changes  $Z(\omega)$  with frequency change and with increased temperature.

Where we note that impedance changes with frequency at temperature (T = 15, 60 °C) are gradual while these changes are more severe in temperature (T = 30 °C). from Figure (21) we found that impedance is inversely proportional to both the applied frequency and the temperature, and at the frequencies the response corresponding to the temperature reaches a value of (Z = 17 K.Ω, T =15°C), and at temperature (Z = 8.02 K.Ω, T = 30 °C), and at (Z = 8.1 K.Ω, T = 60 °C). We note that at temperature (T = 60 °C), the nodular resistance increases, and this is the reason for the formation of conductive crystalline phases of the type (2H, 3R) when molybdenum sulfide is subjected to pressure of the order of (5 tons) when preparing the tablet.

### 3.14 Calculate the activation energy (E<sub>a</sub>) for type (2H/3R) molybdenum disulfide

The high electrical conductivity is associated with low activation energies, so it is necessary to study the activation energy to complete the electrical characterization and to ascertain the potential properties of molybdenum disulfide and to know the causes of its changing behavior. In order to calculate the activation energy E<sub>a</sub>, we plot the frequency changes Ln(f) as a function of the reciprocal of the temperature, and we get The Arrhenus curve shown in Figure (22) and represented by the two relations (5, 6) [9,10]:

$$\Delta \ln \sigma = -\frac{E_a}{k} \times \frac{1}{T}, \sigma = \sigma_0 \times e^{\frac{E_a}{kT}} \quad (5)$$

$$\Delta \ln F = -\frac{E_a}{k} \times \frac{1}{T} \quad (6)$$

Thus we can determine the value of activation energy E<sub>a</sub>

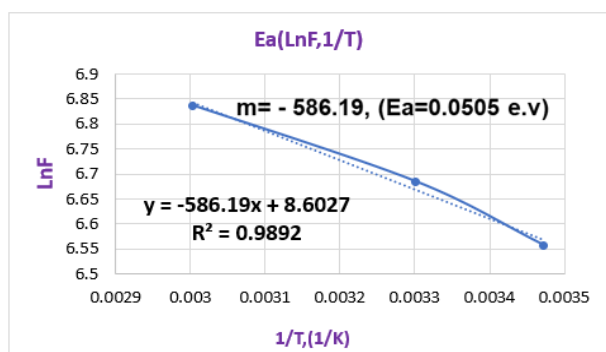


Fig. 22. Arrhenius diagram of LnF frequency variations as a function of the reciprocal temperature variations (1/T).

As the slope of the resulting line in the Arrhenus plot for the studied sample is equal to the activation energy divided by the Boltzmann constant  $m = \frac{E_a}{K}$ , and by substitution we find that

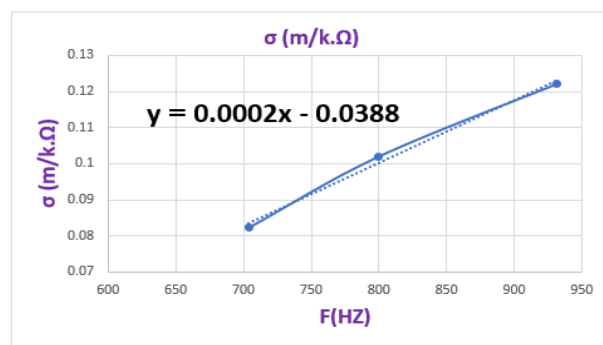
the activation energy is equal to E<sub>a</sub> = 8.089 × 10<sup>-21</sup> (Joul), E<sub>a</sub> = 0.0505 (e.V).

Depending on the results obtained from the study of the impedance spectra, we can calculate some of the internal parameters of the crystallized molybdenum disulfide sample (MoS<sub>2</sub>-2H/3R,Tablet), where the study was carried out under three temperatures (T = 15, 30, 60 °C), and by determining the frequencies that achieve the relation (ω × τ<sub>p</sub> = 1), we were able to determine the following parameters: the resistance of the sample during frequency application, the resistivity of the sample, and the electrical conductivity. These results are arranged in Table (2).

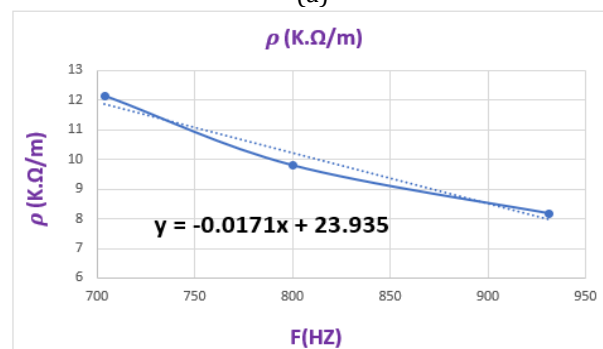
Table 2. Some internal parameters of the studied sample of molybdenum disulfide (MoS<sub>2</sub>-2H/3R -Tablet).

T(°K)	F(HZ)	X(w)(K.Ω)	LnF	ρ (K.Ω/m)	σ (m/k.Ω)
288	704	42.3	6.556	12.139	0.0823
303	800	39.99	6.68	9.803	0.102
333	931	38.68	6.83	8.186	0.122

The changes of resistivity and conductivity with frequency for a sample of crystallized molybdenum disulfide (MoS<sub>2</sub>-Tablet) are expressed through Figure (23).



(a)



(b)

Fig. 23. (a) Variations of conductivity (σ) with peak frequency, (b) Variations of resistivity (ρ) with peak frequency.

### 3.15 Calculating the donor density in (MoS<sub>2</sub>-2H/3R-Tablet)

To calculate the density of electron traps for a sample of molybdenum disulfide (MoS<sub>2</sub>-Tablet), some basic calculations are necessary, which are the dimensions of the Tablet, the area of the tablet, the number of Electric charge carriers, and the number of atoms in the Tablet. The thickness of the tablet is (d = 1.56 m. m), the diameter of the Tablet is (2r = 14 m. m), the area of the Tablet is by calculation it turns out that: A = 153.86 × 10<sup>-6</sup> m<sup>2</sup>, the mass of the disc (M = 1gr), and the volume of the disc V = A × d. By calculation, it was found that V = 240.02 × 10<sup>-9</sup> m<sup>3</sup>. Therefore The density of electric charge carriers in (MoS<sub>2</sub>-2H/3R, Tablet) was calculated from the relationship (7), [10]:

$$N_0 = \frac{M}{V} \times N_a \quad (7)$$

By calculation, it turns out that the number of primordial atoms of the sample is equal to

$$N_0 = (25 \times 10^{26}) \frac{\text{atom}}{\text{m}^3}$$

From the relation (8) that connects the activation energy and temperature

$$N_d = N_0 \times e^{\frac{-E_a}{k.T}} \quad (8)$$

Where T = (15,30,60) °C, K = 1.38 × 10<sup>-23</sup> K Boltzmann constant, and E<sub>a</sub>: activation energy. At temperature (t = 15°C) and by calculation we have: N<sub>d</sub> = 3.27 × 10<sup>26</sup>  $\frac{1}{\text{m}^3}$ , At temperature (t = 30°C) we have: N<sub>d</sub> = 3.62 × 10<sup>26</sup>  $\frac{1}{\text{m}^3}$ , At temperature (t = 60°C) we have: N<sub>d</sub> = 4.308 × 10<sup>26</sup>  $\frac{1}{\text{m}^3}$ , These changes are arranged in Table (3).

**Table 3.** Shows the density of Electric charge carriers with the change of temperature.

T(°C)	15	30	60
N <sub>d</sub> ( $\frac{1}{\text{m}^3}$ )	3.27 × 10 <sup>26</sup>	3.62 × 10 <sup>26</sup>	4.308 × 10 <sup>26</sup>

### 3.16 Calculating the potential barrier height (Ψ) for molybdenum disulfide (MoS<sub>2</sub>-2H/3R -Tablet)

The sample (MoS<sub>2</sub>-Tablet) was heated by placing it in the oven and measuring the electrical resistance. We noticed that the behavior of the resistance is unstable, once increasing and decreasing, so we heated the sample to (T=40°C) and stopped the heating process and while the

temperature was decreasing of (T=40°) to (T=20°C) We took the resistance of the sample as the resistance of the sample (MoS<sub>2</sub>-2H/3R - Tablet) at temperature (T=40C) was (R=30K.Ω), and at temperature (T=21°C) it was R=(93.7)K.Ω, as shown in Figure (24).

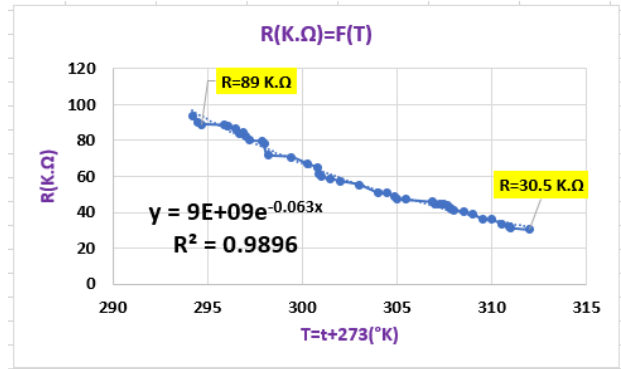


**Fig. 24.** Electrical resistance (R) changes with temperature.

### 3.17 Variation of resistivity (g) with temperature (T)

The resistivity changes with temperature have been plotted, as it is shown that the resistivity decreases with increasing temperature, as shown in Figure (25). It is clear that the qualitative resistance decreases with increasing temperature, as its value is (g = 9.23 k.Ω. m) at (T = 21 °C), and at (T = 40 °C) the value of qualitative is (g = 3.0073 k.Ω. m).

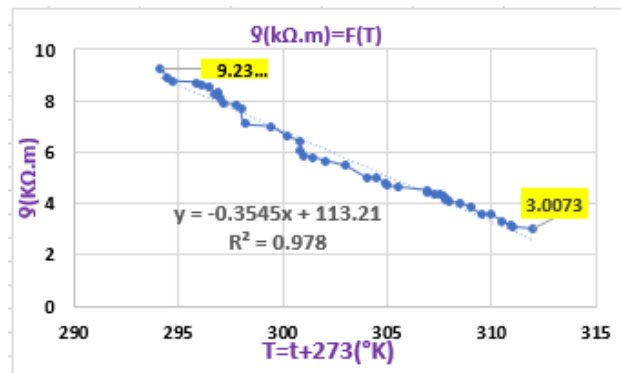


**Fig. 25.** Resistivity changes with temperature.

### 3.18 Calculating the density of electronic traps N<sub>s</sub>

The density of traps or surface states is calculated from the relation (9) [11]:

$$\Psi = \frac{g \times N_s^2}{2 \times \epsilon_0 \times \epsilon_r \times N_d} = \frac{g \times N_s^2}{2 \times \epsilon_t \times N_d} \Rightarrow N_s^2 = \frac{2 \times N_d \times \Psi \times \epsilon_t}{g} \quad (9)$$

Where  $\Psi$  is the height of the potential barrier,  $\epsilon_r$ : is the relative permittivity of molybdenum disulfide,  $\epsilon_0$ : is the vacuum permittivity, and the electron charge  $g = e = 1.6 \times 10^{-19}J$ , and the value of the potential barrier  $\Psi$  in electron volts. Using the calculated value of  $\Psi = 0.494(e.V)$ , we find t1hat the value of the trap density or surface states  $N_s^2 = \frac{2 \times N_{d,t} \times \Psi \times \epsilon_T}{g}$ . And the permittivity calculated from the changes of the dielectric constant with the frequency and We arranged the results in a table (4).

**Table 4.** shows the changes of density of electronic traps  $N_s$  and permittivity with temperature changes.

T(°C)	15	30	60
$\epsilon_t \left(\frac{f}{m}\right)$	$1.048 \times 10^{-8}$	$1.6 \times 10^{-8}$	$1.53 \times 10^{-10}$
$N_s \left(\frac{Trape}{m^2}\right)$	$1.84 \times 10^9$	$2.39 \times 10^9$	$2.55 \times 10^{-10}$

### 3.19 Calculating the width of the barren area

After obtaining the  $N_d$  and  $N_s$ , the width of the stripped area  $X$  at the particle front was calculated, which is given by the relation following:  $X = \frac{N_s}{2N_d}$  [12], and for the different temperatures, we found that at  $T = 15^\circ C$   $X_{T=15^\circ C} = 0.28 \times 10^{-17}$  and for the temperatures  $T=30^\circ C$ ,  $X_{T=30^\circ C} = 0.33 \times 10^{-17}$ , and for the temperatures ( $T=60^\circ C$ ), we found  $X_{T=30^\circ C} = 0.29 \times 10^{-18}$ . We note from the previous results that with the increase in temperature, the density of donor atoms  $N_d$  increases and the density of electronic traps  $N_s$  decreases, and therefore the ratio of the density of donor atoms to the density of electronic traps is very large, and this indicates that the non-linearity factor  $\alpha$  increases with increasing  $N_d$  and decreasing  $N_s$ . All parameters have been deduced the interior of the studied molybdenum disulfide sample (MoS<sub>2</sub>-Tablet), and we arrange the previous parameters in Table (5).

**Table 5.** It shows the internal parameters of the studied molybdenum disulfide (MoS<sub>2</sub>-2H/3R -Tablet) sample.

T(°K)	F(Hz)	$\tau_p$ (sec)	$N_s \left(\frac{Trape}{m^2}\right)$	$N_d \left(\frac{atom}{m^3}\right)$	X(m)
288	704	$2.25 \times 10^{-4}$	$1.84 \times 10^{+9}$	$3.27 \times 10^{+26}$	$0.281 \times 10^{-17}$
303	800	$1.98 \times 10^{-4}$	$2.39 \times 10^{+9}$	$3.62 \times 10^{+26}$	$0.33 \times 10^{-17}$
333	931	$1.7 \times 10^{-4}$	$2.55 \times 10^{+8}$	$4.308 \times 10^{+26}$	$0.29 \times 10^{-18}$

## 4. CONCLUSIONS

1. We note that there is agreement between Zeta-nano measurements and atomic force microscopy (AFM) images in terms of the dimensions of the molybdenum disulfide structures and layers.
2. When measuring the qualitative resistance during the heating process only and without applying an external frequency on a sample (MoS<sub>2</sub>-Tablet), it was found that the qualitative resistance decreases with increasing temperature, as its value is  $g = (9.23)$  k.Ω.m at ( $T = 21^\circ C$ ) and at temperature ( $T=40^\circ C$ ) has a specificity value of  $g = (3.0073)$  k.Ω. m.
3. The high electrical conductivity is associated with low activation energies, so the activation energy was studied from the Arrhenus diagram and found to be equal to  $E_a = 0.0505$  (e.V) in a molybdenum disulfide sample (MoS<sub>2</sub>-Tablet) of type (2H/3R).

4. The fixed part of the changes of the imaginary part of the impedance becomes less valuable with the increase in temperature wein the order  $T = (15,30,60)^\circ C$ ,  $X(\omega) = (48, 41.66, 35.6)$  K.Ω, and when the temperature increases, we notice The shift of the frequency response peaks towards the higher frequencies that achieve the relation ( $\omega \times \tau_p = 1$ ), which means a decrease in the life time of the charge carriers.
5. The changes of the impedance (Z) with the frequency are inverse changes, where the impedance decreases with the increase in the applied frequency, as we note that the changes of the impedance with the frequency at temperature ( $T=15.60^\circ C$ ) are gradual, while these changes are more severe in temperature ( $T=30^\circ C$ ).
6. We also found that the number of Electric charge carriers ( $N_d$ ) increased with increasing temperature, and the number of electron traps decreased, as well as the relaxation time  $\tau_p$  decreased with increasing temperature.

7. The changes of the impedance (Z) with the frequency are between (180 – 8.02) K.Ω, and this is the reason for the formation of crystalline phases of the type (2H, 1T) when molybdenum sulfide is subjected to pressure of the order of (5 tons) when preparing tablet.

#### Acknowledgement:

Authors are grateful to the Editor-in-Chief of (Journal Tribology in Industry) for a critical reading of the manuscript and his valuable comments. We would like to thank Professor Muhammad Anwar is Battal, Professor Lama AlChab, and Professor Fawwaz Kayali for their contribution to the completion of this research.

#### REFERENCES

- [1] R. Akashi et al., "Two-Dimensional valley electrons and excitons in noncentrosymmetric 3R-MoS<sub>2</sub>," *Physical Review Applied*, vol. 4, no. 1, Jul. 2015, doi: 10.1103/physrevapplied.4.014002.
- [2] R. Suzuki et al., "Valley-dependent spin polarization in bulk MoS<sub>2</sub> with broken inversion symmetry," *Nature Nanotechnology*, vol. 9, no. 8, pp. 611–617, Jul. 2014, doi: 10.1038/nnano.2014.148.
- [3] H. Zeng et al., "Optical signature of symmetry variations and spin-valley coupling in atomically thin tungsten dichalcogenides," *Scientific Reports*, vol. 3, no. 1, Apr. 2013, doi: 10.1038/srep01608.
- [4] T. Cheiwchanamngij and W. R. L. Lambrecht, "Quasiparticle band structure calculation of monolayer, bilayer, and bulk MoS<sub>2</sub>," *Physical Review B, Condensed Matter and Materials Physics*, vol. 85, no. 20, May 2012, doi: 10.1103/physrevb.85.205302.
- [5] N. Takahashi and M. Shiojiri, "Stacking faults in hexagonal and rhombohedral MoS<sub>2</sub> crystals produced by mechanical operation in relation to lubrication," *Wear*, vol. 167, no. 2, pp. 163–171, Aug. 1993, doi: 10.1016/0043-1648(93)90321-c.
- [6] H. Al-Hussein, J. Al-Sharr, S. Othman, H. Khamisy, "Study of the electronic, (structural and optical) properties of MoS<sub>2</sub> nanostructures," *Aleppo University Research Journal*, vol. 170, p. 1656, 2023.
- [7] H. Alhussein, J. Q. AlSharr, S. Othman, and H. AlKhamisy, "Study of the electrical and electronic properties of crystalline molybdenum disulfide (MoS<sub>2</sub>-3R) semiconductor nano using alternating current (AC) measurements," *Nanosistemy: Fizika, Himiâ, Matematika*, vol. 14, no. 6, pp. 633–643, Dec. 2023, doi: 10.17586/2220-8054-2023-14-6-633-643.
- [8] S. Sathiyar, H. Ahmad, W. Y. Chong, S. H. Lee, and S. Sivabalan, "Evolution of the Polarizing Effect of MoS<sub>2</sub>," *IEEE Photonics Journal*, vol. 7, no. 6, pp. 1–10, Dec. 2015, doi: 10.1109/jphot.2015.2499543.
- [9] J. Singh and N. K. Verma, "Structural, optical and magnetic properties of cobalt-doped CdSe nanoparticles," *Bulletin of Materials Science/Bulletin of Materials Science*, vol. 37, no. 3, pp. 541–547, May 2014, doi: 10.1007/s12034-014-0671-4.
- [10] P. Vincenzini, *Proceedings of the World Congress on High Tech Ceramics, Technologies* (6th CIMTEC), Milan, Italy, 24-28 June 1986.
- [11] K. Al Abdullah, A. Batal and W. Haj Ismail, "Structural and electrical properties of ZnO embedded in PANI solvent", *Journal of Electron Devices*, vol. 21, pp. 1869 -1873, 2015.
- [12] K. Al Abdullah, S. Awad, "Improving the electrical properties of ZnO varistors using nano powder structures", Ph.D. thesis, Faculty of Electrical and Electronic Engineering, University of Aleppo, 2020.